Genetic variability and structure of the Olive Field Mouse: a sigmodontine rodent in a biodiversity hotspot of southern Chile

Paulo S. Zepeda [Corresp., 1] , Enrique Rodríguez-Serrano [2] , Fernando Torres-Pérez [3] , Juan L. Celis-Diez [4] , R. Eduardo Palma [1]

[1] Laboratorio de Biología Evolutiva, Departamento de Ecología, Facultad de Ciencias Biológicas, Pontificia Universidad Católica de Chile, Santiago de Chile, Chile

[2] Departamento de Zoología, Facultad de Ciencias Oceanográficas y Naturales, Universidad de Concepción, Concepción, Chile

[3] Instituto de Biología, Facultad de Ciencias, Pontificia Universidad Católica de Valparaiso, Valparaiso, Chile

[4] Escuela de Agronomía, Pontificia Universidad Católica de Valparaíso, Valparaiso, Chile

Corresponding Author: Paulo S. Zepeda
Email address: pszepeda@uc.cl

The temperate rainforests of southern Chile, a recognized biodiversity hotspot, were significantly affected by Pleistocene glacial cycles in their southern portion and have been severely disrupted mainly due to recent human activities. Additionally, the landscape is characterized by a series of potential barriers to gene flow, such as the Chacao Channel, Cordillera de Piuche in Chiloé and both the Ancud and the Corcovado gulfs. We used mitochondrial DNA sequences and microsatellite data across several populations to evaluate the genetic variability and structure of the sigmodontine rodent *Abrothrix olivacea brachiotis*, one of the most common species of small mammals and an inhabitant of these biodiverse forests. Sequencing data showed that along with the recovery of high haplotype variation for this species, there was a low nucleotide diversity between haplotypes, showing no genetic differences between the Chiloé Island and continental populations in southern Chile or through any other geographic barrier in the study area. However, microsatellite data exhibited some level of population structuring. The most evident clusterings were those of the Chiloé Island and that of North Patagonia. These findings are corroborated by a barrier analysis that showed a genetic barrier in the latter areas, whereas the Chacao Channel was not a significant barrier for this rodent. Overall, the genetic variability and structure of *A. o. brachiotis* was concordant with historical factors, such as the Last Glacial Maximum and the presence of geographic elements that isolate populations.

1 **Genetic variability and structure of the Olive Field Mouse: a sigmodontine**

2 **rodent in a biodiversity hotspot of southern Chile**

4 Paulo S. Zepeda[1], Enrique Rodríguez-Serrano[2], Fernando Torres-Pérez[3], Juan L. Celis-Diez[4], R.

5 Eduardo Palma[1]

6 [1] Laboratorio de Biología Evolutiva, Departamento de Ecología, Facultad de Ciencias

7 Biológicas, Pontificia Universidad Católica de Chile, Santiago, Chile

8 [2] Departamento de Zoología, Facultad de Ciencias Oceanográficas y Naturales, Universidad de

9 Concepción, Concepción, Chile

10 [3] Instituto de Biología, Facultad de Ciencias, Pontificia Universidad Católica de Valparaíso,

11 Valparaíso, Chile

12 [4] Escuela de Agronomía, Pontificia Universidad Católica de Valparaíso, Valparaíso, Chile

14 Corresponding Author:

15 Paulo S. Zepeda[1]

16 Alameda 340, Santiago, Chile

17 Email address: pszepeda@uc.cl

19   **Abstract**

21   The temperate rainforests of southern Chile, a recognized biodiversity hotspot, were significantly

22   affected by Pleistocene glacial cycles in their southern portion and have been severely disrupted

23   mainly due to recent human activities. Additionally, the landscape is characterized by a series of

24   potential barriers to gene flow, such as the Chacao Channel, Cordillera de Piuche in Chiloé and

25   both the Ancud and the Corcovado gulfs. We used mitochondrial DNA sequences and

26   microsatellite data across several populations to evaluate the genetic variability and structure of

27   the sigmodontine rodent *Abrothrix olivacea brachiotis*, one of the most common species of small

28   mammals and an inhabitant of these biodiverse forests. Sequencing data showed that along with

29   the recovery of high haplotype variation for this species, there was a low nucleotide diversity

30   between haplotypes, showing no genetic differences between the Chiloé Island and continental

31   populations in southern Chile or through any other geographic barrier in the study area.

32   However, microsatellite data exhibited some level of population structuring. The most evident

33   clusterings were those of the Chiloé Island and that of North Patagonia. These findings are

34   corroborated by a barrier analysis that showed a genetic barrier in the latter areas, whereas the

35   Chacao Channel was not a significant barrier for this rodent. Overall, the genetic variability and

36   structure of *A. o. brachiotis* was concordant with historical factors, such as the Last Glacial

37   Maximum and the presence of geographic elements that isolate populations.

38

39   Introduction

40

41   The temperate rainforest of South America, mostly in Chile, is one of the largest areas of

42   forests in the southern hemisphere and is rich in endemic species (Veblen 2007). The region has

43   also been named one of the 200 most important ecoregions by the World Wildlife Fund (WWF)

44   due to the biodiversity, endemism (particularly for plants) and degree of threat (Olson and

45   Dinnerstein 1998). These forests have been included within the 34 hotspots of biodiversity in the

46   world (Mittermeier et al. 2004). Approximately 45% of the pre-Columbian forest cover has been

47   lost due to human activities (Miranda et al. 2016), being mainly replaced by crops, exotic

48   forestry plantations (e.g., Pinus radiata and Eucalyptus spp), firewood extraction, overgrazing

49   and recent fires (Cavelier and Tecklin 2005; Echeverria et al. 2007; Lara et al. 2012; Bowman et

50 al. 2019). Of note, the percentage of forest loss is stronger between 39 º to 41 º S in Chile,

51 reaching its lowest value at 42 º S in the northern portion of Chiloé Island. In addition, the type

52 of vegetation replacement is different between the continent and the latter island, with more

53 exotic tree plantations in the mainland and more shrublands in Chiloe.

54   Historical processes have modified the landscape, creating geographic barriers among

55 populations and changes in population sizes. Among these barriers, there are the Piuche

56 mountain range in Chiloé Island and the Gulf of Ancud and the Gulf of Corcovado that separates

57 the island from North Patagonia. Alternatively, the Pleistocene glacial cycles affected an

58 important area of the landscape in the Americas, particularly the southern cone of South

59 America. Historical records show that the temperate rainforests of the Cordillera de la Costa in

60 Chile played a central role in maintaining higher endemism, species and genetic diversity.

61 Because the southern portion of South America was severely affected by the Pleistocene glacial

62 cycles (Holling and Schilling 1981, Harrison 2004), the geographical ranges of several species

63 associated with temperate rainforests were restricted due to climatic changes triggered by

64 glaciations. The survival of most species was restricted to small areas of oceanic influence

65 known as "refugia." In fact, several refuge areas have been recognized in coastal areas of south-

66 central Chile, both for plants and animals (Villagrán and Hinojosa 1997, Sérsic et al. 2011,

67 Segovia et al. 2012).

68   Within small mammals, the sigmodontine rodents (Cricetidae) are one of the most

69 important inhabitants of the Chilean temperate rainforests, including *Abrothrix olivacea* (the

70 "olive field mouse"), one of the most abundant and characteristic rodents of this biome. The

71 species ranges from 18 to 54º S (Mann 1978; Osgood 1943; Patterson et al. 2015), encompassing

72 areas of the Coastal Desert, the Mediterranean, the Valdivian and the Patagonian Forests and

73 steppe. A former phylogeographic study reported strong structuring for the species, recognizing

74 seven subspecies (Mann 1978), including *Abrothrix olivacea brachiotis* restricted to the

75 temperate rainforests of southern Chile, from Valdivia (39º S) southward to Aysén (45º S),

76 including the Chiloé Island and southern archipelagoes nearby (Osgood 1943; Pearson and Smith

77 1999; Rodríguez-Serrano et al. 2006; Patterson et al. 2015). The home range of *A. olivacea* in

78 southern Chile is approximately 730 to 2530 m^2 (González et al. 1982), which is considered high

79 for a small rodent (25 g average for adult forms). The subspecies brachiotis is found in diverse

80 types of habitats from grasses to shrubs and humid forests (Iriarte 2008). This subspecies is also

81   found in Chiloé Island, regardless of the potential barrier that constitutes the Chacao Channel

82   (widest portion 4.6 km and narrowest part 1.8 km). The results of nucleotide sequence analyses

83   found no genetic differences between specimens from Chiloé (Northern part) and mainland areas

84   (Rodríguez-Serrano et al. 2006). The latter pattern has also been reported for other sigmodontine

85   mice, such as *Abrothrix manni* (D'Elía et al. 2015), the pygmy rice-rat or long-tailed mouse

86   *Oligoryzomys longicaudatus* (Palma et al. 2005, 2012), and the microbiotheriid mouse opossum

87   Dromiciops gliroides (Himes et al. 2008). The opposite pattern (i.e., differentiation between the

88   continent and the island) has been reported for other species, such as the small cervid *Pudu puda*

89   (Fuentes-Hurtado et al. 2011), Darwin's fox *Pseudalopex fulvipes* (Vilà et al. 2004; Yahnke et al.

90   1996), and even for an iguanid lizard, *Liolaemus pictus* (Vidal et al. 2012). *Leopardus guigna*

91   follows the same differentiation pattern of *Abrothrix olivacea*, at the subspecies level, when

92   analyzed with mitochondrial sequences. However, further analyses with microsatellite data

93   showed genetic structuring, recovering a Chiloe and a continental cluster, with the Chacao

94   Channel creating a recent barrier to gene flow (approximately 8,000 years before present;

95   Napolitano et al. 2014). The latter scenario questions whether the use of a more sensitive

96   molecular marker, such as microsatellites, can unveil a barrier condition for the Chacao Channel.

97   The information regarding genetic patterns of variability and structuring in the temperate

98   rainforest of Chile has been mainly sourced by mitochondrial sequence analysis. The use of more

99   variable markers such as microsatellites will provide valuable and sensitive data from a genetic

100   scope (Frankham 1996; Frankham et al. 2002). With this type of marker, we can study patterns

101   that may not be resolved with more conserved regions of DNA and will allow us to test for

102   genetic variability and structure on a finer scale and from recent historical processes.

103   Using microsatellite and mitochondrial sequence data along several populations from

104   both continental and island (Chiloé) areas of southern Chile, we evaluated the genetic variability

105   and structuring of *Abrothrix olivacea brachiotis* along its distribution in the temperate rainforests

106   of southern Chile. In addition, we evaluated the potential effects of existing geographic barriers

107   in the geographic distribution of *A. o. brachiotis*, such as the Chacao Channel, the Piuché

108   Mountains in Chiloé Island, and the border of the LMG. The ecological and evolutionary

109   features of *A. olivacea* populations, coupled with the hotspot of biodiversity where this species

110   lives, provides a useful model for examining historical and ecological processes that shape the

111   genetic variability and population structure of *A. o. brachiotis*.

112

113   Methods

114

115   Sample collection

116

117   The study area encompasses the complete geographic distribution of the subspecies *Abrothrix*

118   *olivacea brachiotis*, between Los Rios (40 ºS) and Aysen (45 ºS) regions in the temperate

119   rainforest ecoregion (green shade with black stripes, Fig. 1). We sampled 11 localities with at

120   least 2 sampling points, except for Chiloé National Park (Cucao), which had a single site (Fig. 1;

121   see Table S1 for sampled localities). The sampling gap between the southernmost localities on

122   the continent was due to the geographic difficulties in accessing that area for fieldwork.

123

124   Most of the tissues used in this study were retrieved from *A. o. brachiotis* voucher

125   specimens deposited in the Colección de Flora y Fauna "Profesor Patricio Sánchez Reyes"

126   (SSUC), Departamento de Ecología, Pontificia Universidad Católica de Chile, Santiago, Chile,

127   and in the Museum of Southwestern Biology (MSB), Department of Biology, University of New

128   Mexico, Albuquerque, New Mexico, USA. The remainder of the samples were the result of field

129   campaigns in which standard Sherman traps were used (8 × 9 × 23 cm; H. B. Sherman Traps,

130   Inc., Tallahassee, FL, USA) with oats and vanilla as bait. Fieldwork protocols followed the

131   standard bioethical and biosafety protocols outlined by the American Society of Mammologists

132   (ASM; Sikes and Gannon 2011), and the Centers for Disease Control and Prevention (CDC;

133   Mills et al. 1995), respectively. All of the new rodent captures were deposited at SSUC. The

134   captures were conducted under the Chilean Government authorization (Servicio Agricola y

135   Ganadero; SAG): Resolución Exenta #5675/2013 and the approval of the Bioethics Committee

136   of Pontificia Universidad Católica de Chile (#CBB-220/2012). A detailed list of specimens

137   sequenced per locality is given in Table S1. A total of 187 samples were used in this study. All

138   of them were genotyped for microsatellite loci, and a subset of 107 samples was sequenced for

139   the mitochondrial hypervariable region I (HVI) analyses (see Table S1 for samples sequenced

140   and genotyped).

141

142   Laboratory procedures

143 DNA Extraction

144

145 DNA was extracted from either frozen tissues (- 80˚C) or ethanol preserved tissues (liver, lung or

146 kidney) using the Wizard Genomic DNA Purification Kit (PROMEGA, Madison, Wisconsin) or

147 the Phenol-Chloroform protocol (modified from Sambrook, Fritsch & Maniatis, 1989).

148

149 Mitochondrial DNA

150 Through the polymerase chain reaction (PCR), we amplified the complete hypervariable domain

151 I (HVI) of the mtDNA control region, using primers and protocols outlined in Rodríguez-Serrano

152 et al. (2006). A total of 483 base pairs (bp) of the HVI region from 92 individuals were

153 sequenced and then deposited at the GenBank database (accession numbers: MH714355 to

154 MH714446). In addition, another 15 sequences of the subspecies Abrothrix olivacea brachiotis

155 were obtained from GenBank (Accession numbers: AY840064 to AY840078). We thus

156 completed a total of 107 sequences that were aligned using the Clustal W program (Larkin et al.

157 2007) implemented in the software BIOEDIT (Hall 1999). All samples were sequenced in

158 MACROGEN Inc. (Seoul, Korea).

159

160 Microsatellite DNA

161 A total of 28 microsatellite primer pairs were specially designed for this study through the

162 company Genetic Marker Services Laboratories (London, UK). Following the manufacturer's

163 instructions, we standardized only those that presented good quality in the report given by the

164 company. A subset of 16 SSR was screened for polymorphisms and then tested for genotyping

165 problems in Microchecker (van Oosterhout et al. 2006). After these tests, 12 loci were the final

166 set of primers used in this study (Table S2). Using the program FSTAT version 2.9.3.2 (Goudet

167 1995), we tested for linkage disequilibrium between pairs of loci. PCR conditions were

168 standardized specifically for these newly designed primers with a protocol in a 10 µl reaction

169 volume containing 2 µl of Buffer 5X, 2 µl of MgCl2 at 25 µg/µl, 1 µl of dNTPs at 2 µg/µl, 0.25

170 µl of BSA, 0.2 µl of forward primer and 0.2 µl of reverse primer, 0.35 µl of M13 fluorescence

171 tail, 0.15 µl of Taq polymerase, and finally 2 µl of DNA at 40 ng/µl. Each pair of primers was

172 standardized to a thermocycler protocol with 32 cycles of 1 min denaturation at 95 ºC, annealing

173 of 1 min – 2 cycles each 65-59 ºC, 10 cycles at 58 ºC, 10 cycles at 57 ºC, an elongation of 1 min

174 at 72 ºC, and a final extension at 72 ºC for 5 min (Table S2).

175 Microsatellites were fragment analyzed in an ABI3500 and then genotyped with the software

176 GENEMAPPER (GeneMapper® v4.0; Applied Biosystems®, Foster City, CA, USA). In the

177 standardization process, at least 8 samples of different localities were repeated to ensure

178 consistency in the genotyping process. Additionally, the dataset was analyzed with the software

179 Microchecker (van Oosterhout et al. 2006) for testing allelic dropout and null alleles.

180

181 Analyses of genetic structure and variability

182

183 Mitochondrial DNA

184

185   To examine population dynamics, we used Tajima's test of neutrality (Tajima 1989). Assuming

186 that sequence variation in the control region was neutral, we calculated the Tajima's D index to

187 test the occurrence of population expansion if the values obtained indicated a significant negative

188 value or a population equilibrium. To assess the population structure, a median-joining haplotype

189 network was generated based on the HVI sequence dataset, using the software popART 1.7

190 (Leigh & Bryant 2015; Bandelt 1999). The graph was calculated and plotted using the median-

191 joining algorithm. Genetic diversity and variability were measured calculating haplotype (Hd)

192 and nucleotide (π) diversity using popART 1.7 (Leigh & Bryant 2015; Bandelt 1999) (Table 1).

193

194 Microsatellite DNA

195 Genetic diversity indexes were calculated with the software GENODIVE (Meirmans and

196 Tienderen 2004) and HPrare (Kalinowski 2005). We thus calculated the observed and expected

197 heterozygosity, the number of alleles (A) and the number of alleles standardized to the

198 population with the smallest sample size (Ar). Additionally, with the software NeEstimator (Do

199 et al. 2014), we estimated the effective population size (Ne) for each of the clusters calculated

200 with the Structure software (see below) using the linkage disequilibrium method (Hill

201 1981;Table 1). Deviations from the Hardy-Weinberg equilibrium were examined for each

202 population at each locus calculating the fixation index Fis with the software GENODIVE.

203 Genetic differentiation was assessed with pairwise Fst values between populations (Table S3).

204 Isolation by Distance (IBD) was calculated through a Mantel test with GenAIEx software (v6.5;

205 Peakall and Smouse 2012). To run this program, we generated a geographic distance matrix and

206 a Nei's Index for obtaining a genetic distance matrix. Significance was tested using 9,999

207 permutations.

208 We used the Structure software (Prichard et al. 2000) to define population genetic

209 structure without assuming a priori knowledge of sampling location or number of populations.

210 To determinate the number of clusters, we used 10,000,000 iterations with a burn-in of 1,000,000

211 simulations. We evaluated K among 1 to 8 clusters, and each was run 10 times to ensure the

212 stability and variance of likelihood values. Admixture and correlation models were used. These

213 models assume mixed ancestry for all analyzed individuals and where the allele frequencies of

214 closely related populations may be correlated. To determine the most likely K of our sample, we

215 used the approach of Evanno implemented in the web platform Clumpak (Kopelman et al. 2015)

216 (Evanno et al. 2005). In this platform, the second-order rate of change of the log probability of

217 data with respect to the number of clusters was examined. The same platform delivers a graphic

218 and color representation that combines runs.

219 We performed GENELAND analyses (Guilliot et al. 2005) considering the microsatellite

220 genetic data plus the spatial location of samples. This approach is a Bayesian cluster analysis that

221 uses individual geo-referenced genetic data to detect the number and geographic position of

222 populations (Guilliot et al. 2008). The algorithm identifies genetic discontinuities while

223 estimating both the number and locations of populations without any a priori knowledge on the

224 population units and limits. Once the number and limits of populations were established, the

225 population membership probability was calculated from the posterior probability distribution of

226 the MCMC. First, one independent run was performed by 10,000,000 iterations, sampling every

227 1,000 iterations of the Markov Chain and treating the number of populations as unknown varying

228 between K= 1 to 8. Then, we chose the better of 20 independent runs, each of 10,000,000

229 generations and sampling every 1,000 but now treating the number of populations as a fixed

230 parameter estimated from the first independent run. We used the admixture model and correlated

231 allele frequencies to estimate the posterior probability of the data with 1 km of uncertainty to

232 detect possible different clusters of samples with shared localities. From the posterior

233 distribution, we drew a map of probability isoclines of population membership, one for each

234 population or cluster inferred by the model. With this result, a map with the geographic limit was

235   elaborated using QGIS (QGIS Development Team (2019). QGIS Geographic Information

236   System. Open Source Geospatial Foundation Project. http://qgis.org).

237   The software Barriers (vs 2.2, Manni et al. 2004) was used to test the occurrence of

238   genetic barriers between different localities. This program uses a Monmonier's algorithm with

239   Delaunay triangulation. The significance of a detected barrier is the result of 1000 sub replicates,

240   and the matrices of pairwise differences were generated by the software MSAT (Dieringer &

241   Scholotterer 2003). For this analysis, a barrier was considered valuable when we obtained

242   bootstrap values over 90% (Fig. 1).

243

244   Results

245   Mitochondrial DNA Data Analysis

246   The haplotype gene diversity (Hd) was 0.965 (variance 0.00007), the nucleotide diversity (Pi)

247   was 0.01070, and the Tajima index calculated over the mitochondrial data showed a value of -

248   1.84 (0.1 p > 0.05), which is not significant, meaning that populations exhibited neutrality.

249   The median-joining network recovered 56 haplotypes (Fig. 2) for the 107 mtDNA

250   sequences of the HVI mtDNA region. Figure 2 shows a group of haplotypes of low frequency

251   and few mutational steps (between 1-3) from Cucao ("purple") in Chiloé Island. Another

252   clustering of haplotypes ("red") was observed with samples from Senda Darwin Biological

253   Station in the north of Chiloé Island. Some of these haplotypes exhibited high frequencies with

254   up to 8 sequences but with low mutational steps (the highest with 5 steps). There is a shared

255   haplotype of high frequency (13 sequences) that recovered localities from the mainland and the

256   Chiloé Island. In addition, the Valdivian localities had haplotypes that spread throughout the

257   network; these haplotypes were of low frequencies, with few mutational steps (1-3) and related

258   to localities of Mininco and Río Blanco in the southernmost distributional range of *A. o.*

259   *brachiotis* in northern Patagonia. At this latter point, a high frequency haplotype (11 sequences)

260   was recovered that included the two latter localities of Mininco and Rio Blanco. Other

261   haplotypes ("turquoise," "gray" and "green;" see legend Fig. 2) represent north-continental

262   localities that are connected among them with few mutational steps and low frequencies.

263

264   Microsatellite data analysis

265   Results from Microchecker showed that loci Aol44, Aol55B, Aol91 and Aol52B deviated from

266   Hardy-Weinberg equilibrium with heterozygosity deficiency. This was the case for only a single

267   population per locus, and for this reason, data were not removed from the analysis. None of the

268   populations revealed heterozygosity excess, and Microchecker did not identify genotyping

269   errors, null alleles, or allele dropout in our data. There was no significant genotypic linkage

270   disequilibrium detected for any pair of loci.

271   In Table 1, we show the genetic diversity for microsatellite data per localities. We

272   considered 11 populations and pooled Palena with Santa Lucia due to the geographic proximity

273   of the size of these two populations. Ho and He were similar except in La Picada, but this may be

274   due to the low sample size. The FST index calculated between all populations gave a majority of

275   significant differences between populations with the exception of La Picada vs. the rest, but this

276   may also be due to a low sampling size. Additionally, the Mantel correlation coefficient, the test

277   for isolation by distance, was positive (Rxy = 0.386, p = 0.01; Figure 3), giving a positive and

278   significant correlation between genetic and geographic distance.

279   We observed that the highest number of alleles was concentrated between the mainland

280   and Senda Darwin Biological Station in Chiloé, although the Cucao and North-Patagonian

281   populations also concentrated an important number of alleles. The effective number of alleles

282   (corrected with the sample size) was higher in the continent than in Chiloé Island and North-

283   Patagonian populations. The same Table 1 shows no significant differences between observed

284   and expected heterozygosity values for all localities, showing high values (all of them near 0.8);

285   Gis values were significant for all 4 localities.

286   Figure 4 shows the results of STRUCTURE analysis. The Evanno method (Evanno et al.

287   2005) recovered five clusters (K = 5) with the highest probability (Fig. 4C). From north to south,

288   clusters 1 and 2 grouped populations from Panguipulli, Valdivia, Bahía Mansa, La Picada and

289   Las Quemas ("purple" and "yellow"); cluster 3 ("blue") included mainly populations from Senda

290   Darwin Biological Station (north of Chiloé Island); cluster 4 ("orange") constitutes the Cucao

291   population (central Chiloé at Chiloé National Park), and the last cluster ("green") included

292   southern populations of Palena, Santa Lucía, Río Simpson, Mininco and Alto Río Ibañez in

293   North Patagonia. Clusters 1 and 2 ("yellow" and "purple") recovered an intermingling of

294   probabilities for continental populations from the northernmost distribution of *A. o. brachiotis,*

295   from Panguipulli to Las Quemas. However, some individuals from Panguipulli were assigned to

296   the orange cluster. The second highest supported ΔK recovered 3 clusters (Fig. 4A), identifying

297   the same clusters showed in K = 5: "blue," "orange" and "green," whereas individuals from the

298   continent (clusters "yellow" and "purple") were assigned to clusters "orange" and "blue." We

299   also show analysis with K = 4, exhibiting the same pattern, with coastal south temperate forest

300   populations forming a not well defined cluster, two clusters in Chiloé Island, and another

301   grouping the populations of North Patagonia.

302   Even though K=5 clusters with the highest probability, K=4 has greater biological sense.

303   Following this finding, we estimated the effective size of K= 4 obtained with Structure

304   (Continental, Senda Darwin, Cucao and North Patagonia). The biggest effective size was in the

305   continent with 683.3, followed by Senda Darwin with 274.9; the smallest cluster was Cucao with

306   54 individuals. In the mainland, the top limit of the confidence interval is infinite (Table 1).

307   The population structure for *A. olivacea brachiotis* was also evaluated using the

308   GENELAND v. 1.0.7 program. This analysis inferred three genetic clusters in the study area. A

309   first cluster (Fig. 5A) mostly grouped individuals representing localities of continental Chile and

310   the northern portion of the Chiloé Island. A second cluster joined individuals representing

311   localities of Panguipulli and Cucao (Fig. 5B), and a third cluster grouped all southernmost

312   populations (Fig. 5C). All clusters presented 0.65 of probability in the isocline that grouped the

313   populations.

314   The program Barriers corroborated the genetic isolation of clusters by barriers. In fact, a

315   strong barrier is hypothesized between populations of North Patagonia and the rest of brachiotis'

316   distribution with 100% of appearance with 1000 replicas, and a second barrier was proposed in

317   Chiloé Island between Senda Darwin Biological Station and Cucao. Both proposed barriers

318   exhibited high levels of consistency when we performed the analysis with 1000 replicates.

319

320   Discussion

321

322   Using both mitochondrial and microsatellite markers, we evaluated the structuring and variability

323   across the distribution of *Abrothrix olivacea* in the temperate rainforests of Southern Chile. Our

324   results corroborated the phylogeographic study of Rodriguez-Serrano et al. (2006), which

325   showed no difference when comparing populations of *A. o. brachiotis* between Chiloé Island and

326   the mainland using mitochondrial sequences. In the present study, we recovered two new

327   haplogroups, one in the south of Chiloé (Cucao) that shares haplotypes with the continent, and

328   the North Patagonia haplogroup that included populations of Mininco and Alto Rio Ibañez

329   (ARI). The last haplogroup had one shared haplotype between Valdivia (Northern continental

330   distribution) and Mininco, and few mutational steps with other Valdivian haplotypes. In

331   summary, the mitochondrial analysis showed low genetic structuring for the subspecies

332   brachiotis and the nonoccurrence of exclusive haplotypes for any of the localities and recovered

333   shared haplotypes with North continental localities. The overall mtDNA network had low

334   nucleotide diversity, meaning that besides the high number of haplotypes (high haplotype

335   diversity), there were little differences between them.

336   The Microsatellite Genetic diversity indices showed that across all populations sampled

337   (11), there were no significant differences and that Ho versus He was similar with the exception

338   of La Picada, although this may be due to small sample size. The pairwise Fst showed that only

339   close localities did not show significant differences, such as Mininco with Rio Simpson in North

340   Patagonia. This finding is consistent with the pattern of isolation by distance found in the data.

341   Additionally, the La Picada population, when compared with other localities, did not show (in

342   general) significant differences, most likely due to small sample size.

343   In general, the number of alleles standardized for the sample size revealed that across

344   populations, they all have similar values of allelic richness (7.20-10.45). The only population

345   that exhibited a lower number of alleles was La Picada (4.33). When populations were grouped

346   into 4 clusters (Continental, Senda Darwin, Cucao and North Patagonia), the difference was even

347   smaller (8.70-10.53). Senda Darwin in Chiloé had the lowest allelic richness and the continental

348   groups had the highest. This fact may be due to the recent separation of this population (Senda

349   Darwin) from the continent. High continental allelic richness may explain the different sources

350   of alleles: more than one refuge represents the genetic diversity of this cluster. In fact, this cluster

351   also exhibits the highest number of private alleles. In the case of *A. o. brachiotis*, we did not find

352   a heterozygosity deficit in any of the localities, as there were no significant differences when

353   comparing mainland and island populations. Thus, it seems that despite recent intense forest

354   fragmentation and degradation (Echeverría et al. 2006), the habitat for *A. o. brachiotis* does not

355   seem to be a critical factor for the genetic variability, as it can adapt to new vegetational types to

356   preserve heterozygosity (Murúa and González 1982; Murúa & González 1986; Patterson et al.

357   1990; González et al. 2000).

358   Microsatellite data analyzed across *A. o. brachiotis*'s geographic range recovered five
359 genetic clusters with Structure, with those results having the highest probability through the
360 Evanno method. Two of these clusters corresponded to populations from the mainland, two
361 others corresponded to populations from Chiloé Island, and a single cluster was restricted to the
362 southernmost limit of the subspecies range in the North Patagonian forests (Aysen region). The
363 clusters recovered in the continent ("yellow" and "purple;" Fig. 4c) were not well defined, and
364 individuals were not assigned to a single cluster. They had mixed probabilities belonging to one
365 or another cluster ("yellow" or "purple"), suggesting that these populations maintained their
366 genetic variation and served as a source of alleles for other clusters (Omote et al. 2012). In an
367 LGM scenario, particularly during the interglacial period, coastal refugees and dispersalist
368 populations of iced eastern localities may have dispersed back to central depression and pre-
369 Andean areas in southern Chile (e.g., Panguipulli area). This may have allowed the intermingling
370 of coastal and eastern populations as suggested by the pattern of the current Structure analysis
371 (Sérsic et al. 2011). The pattern of structure for the mainland agreed with the high allelic richness
372 and number of private alleles, due to the composition of genetic diversity of the area, on which
373 more than one refugia has been recognized, which might suggest the source of variation.
374   The structuring of *A. o. brachiotis* within Chiloé is more evident. We recognized two
375 genetic clusters in the island, one represented by the northern population of Senda Darwin
376 Biological Station, and the other represented in the west-central portion of the island, the Chiloé
377 National Park at Cucao. These genetic structures of *A. o. brachiotis* in Chiloé might be explained
378 by different but not mutually exclusive causes, such as the Cordillera de Piuché (a portion of the
379 Coastal Cordillera that separates the Chiloé National Park from the northernmost portion of the
380 island where the Senda Darwin Biological Station is located), and the major town of Castro
381 (Chiloé's capital city) towards the east of the Coastal Cordillera. Other additional barriers that
382 might have isolated the Cucao area from the rest of the island are historical events, such as the
383 glacial border of the LGM during the Pleistocene that advanced throughout the island. This
384 glacial border left a refuge area in northwest Chiloé where a portion of the National Park is
385 located (Rabassa and Claperton 1990, Moreno et al. 2015; Fig. 1). These current and historical
386 factors might have contributed to the existing genetic structure of A. o. brachiotis populations
387 within the island. To the southeast of Chiloé, in the mainland, the North Patagonian structuring
388 of Abrothrix in Palena and Aysén may be explained by isolation by distance: their geographic

389   isolation with respect to Chiloé, and the geographic distance with respect to mainland

390   populations located to the north. These facts, coupled to the glaciation of the LGM that

391   completely covered these populations, might have forced *A. o. brachiotis* to find refuge areas

392   separated from other populations.

393   The effective size of the different clusters is consistent with the size of the localities. We

394   have the largest population in the mainland cluster that has a wide range of sampling points.

395   Moreover, Cucao is estimated as the smallest Ne and is the population that shows the sharpest

396   isolation, with the Piuche Mountains on one side, and the condition of glacial refugia. Of note,

397   the analysis estimated that the continental cluster has the highest effective size. However, its

398   upper limit as infinite could be due to a large effective size, or a limitation of our dataset,

399   considering that this cluster is the largest, and it may need a more exhaustive sampling.

400   Geneland analyses, on the other hand, recovered 3 clusters. One cluster is shared by

401   populations of the continent and Senda Darwin Biological Station in Chiloé Island. This cluster

402   sustains the hypothesis that the Chacao Channel is a recent barrier for *Abrothrix* since the sea

403   level descended during LGM, allowing for a glacial bridge between Chiloé and the continent,

404   generating a refuge area in the coast of the Chile Lake district (Sérsic et al. 2011). Genetic

405   connectivity between Chiloé and the continent have been inferred for other mammals, such as

406   the microbiotheriid mouse opossum *Dromiciops gliroides* (Himes et al. 2008), the long-tailed

407   sigmodontine mouse *Oligoryzomys longicaudatus* (Palma et al. 2012), the sigmodontine

408   *Abrothrix manni* (D'Elía et al. 2015), and even the iguanid lizard *Liolaemus pictus* (Vidal et al.

409   2012a; b). Geneland also recovered two different cluster populations in the island, one to the

410   north of Chiloé (Senda Darwin) and the other in central west Chiloé (Cucao), consistent with the

411   results of Structure. The latter agreed with the hypothesis of refuge for Cucao and the effective

412   barrier that constitutes the Piuché Mountains. Finally, the third cluster is the same that Structure

413   analysis recovered for North Patagonia populations.

414   Finally, the Barrier analysis (Manni et al. 2004) corroborated the occurrence of a genetic

415   barrier due to the Cordillera de Piuché in Chiloe. The same analysis hypothesized the existence

416   of a barrier between North Patagonia populations and the rest of brachiotis' distribution. Both

417   barriers might also be inferred with Structure analysis (a distinctive cluster for northern Chiloé,

418   Cucao and North Patagonia) and with Geneland, which show clusters that are separated by the

419   aforementioned barriers. The Barrier analysis also demonstrated that the Chacao Channel would

420   not be a genetic barrier for *A. o. brachiotis*, and these results are consistent with those of

421   Geneland (Fig. 5A)

422

423   Conclusions

424

425   In this study, we obtained a subtle structuring of populations at the northern portion of the

426   continental range of *A. o. brachiotis*, which is more evident in Chiloé with two major clusters

427   within the island. An additional structuring was recovered in the northern portion of the

428   Patagonian range of *A. o. brachiotis*. Our results seem to suggest that *A. olivacea* and particularly

429   *A. o. brachiotis* restricted to the temperate rainforests of southern Chile, reacts more to historic

430   than to ecological events regarding its genetic population dynamics and that interruptions of

431   connectivity (Chacao Channel) would not constitute a genetic barrier for this rodent. The genetic

432   structuring observed would respond to the geographic and long dated isolation of populations, as

433   observed by the presence of Cordillera de Piuché that isolated populations in north Chiloé (Senda

434   Darwin) with respect to those of Parque Nacional Chiloé (Cucao). In addition, populations from

435   the latter geographic area are located in what was a glacial refuge during the Pleistocene. North

436   Patagonian populations, on the other hand, may constitute a genetic clustering due to their

437   isolation with respect to Chiloé populations and the geographic distance from the northern range

438   of this subspecies. This isolation might be enhanced by geographic barriers, such as both the

439   gulfs of Ancud and Corcovado and the mountain range of the Andes.

440

441   **Acknowledgments**

442

443   We acknowledge the laboratory support of R. A. Cancino and M. P. de Castro from the

444   Laboratorio de Biología Evolutiva (Departamento de Ecología, P. Universidad Católica de

445   Chile), and G. Peralta from the Laboratorio de Diversidad Molecular (CONYCIT –

446   FONDEQUIP EQM150077; same Department) for her support with the genotyping analyses.

447   This paper contributes to the research program of the Senda Darwin Biological Station (Chilean

448   LTSER Network).

449

450   **References**

451

452   Bandelt, H.J.; Forster, P.; Röhl, A. (1999) Median-joining networks for inferring intraspecific

453   phylogenies. Mol Biol Evol 16:37- 48

454   Bowman, D,M,J.S.; Moreira-Muñoz, A.; Kolden, C.A.; Chávez, R.O.; Muñoz, A.A.; Salinas, F.;

455   González-Reyes, Á.; Rocco, R.; de la Barrera, F.; Williamson, G.J.; Borchers, N.;

456   Cifuentes, L.A.; Abatzoglou, J.T. & Johnston, F.H. (2019) Human-environmental drivers

457   and impacts of the globally extreme 2017 Chilean fires. Ambio. 48:350.

458   Cavelier, J. & Tecklin, D. (2005) Conservación de la cordillera de la costa: Un desafio urgente

459   de la ecoregión valdiviana (pp. 632-641). In: Smith, C.; Ramírez, C.; Armesto, J. &

460   Valdovinos, C., editors. Historia, 23 biodiversidad y ecología del bosque costero de

461   Chile. Editorial Universitaria, Santiago, Chile.

462   D'Elía, G.; Teta, P.; Upham, N.S.; Pardiñas, U.F.J. & Patterson, B.D. (2015) Description of a

463   new soft-haired mouse, genus *Abrothrix* (Sigmodontinae), from the temperate Valdivian

464   rainforest. J Mammal. 96: 839-853.

465   Dieringer, D. & Schlötterer, C. (2003). Microsatellite analyser (MSA): a platform independent

466   analysis tool for large microsatellite data sets. Mol Ecol Notes. 3: 167-169.

467   Do, C.; Waples, R.S.; Peel, D.; Macbeth, G.M.; Tillet, B.J. & Ovenden, J.R. (2014) NeEstimator

468   V2: reimplementation of software for the estimation of contemporary effective population

469   size (Ne) from genetic data. Mol Ecol Resour. 14:209-214.

470   Echeverría, C.; Newton, A. C.; Lara, A.; Benayas, J. M. R. & Coomes, D. A. (2007) Impacts of

471   forest fragmentation on species composition and forest structure in the temperate

472   landscape of southern Chile. Global Ecol Biogeogr. 16: 426-439.

473   Evanno, G.; Regnaut, S. & Goudet, J. (2005) Detecting the number of clusters of individuals

474   using the software structure: a simulation study. Mol Ecol. 14: 2611-2620.

475   Frankham, R. (1996) Relationship of genetic variation to population size in wildlife.

476   Conservation Biology, 10: 1500–1508.

477   Frankham, R.; Ballou J.D. & Briscoe, D.A. (2002) Introduction to Conservation Genetics.

478   Cambridge University Press, Cambridge.

479   Fuentes-Hurtado, M.; Marín, J.C.; González-Acuña, D.; Vergudo, C.; Vidal, F. & Vianna, J.

480   (2011) Molecular divergence between insular and continental Pudu deer (*Pudu puda*)

481   populations in the Chilean Patagonia. Stud Neotrop Fauna E. 46: 23-33.

482 González, L.A.; Murúa, R. & Feito, R. (1982) Densidad poblacional y padrones de actividad
483   espacial de *Akodon olivaceus* (Rodentia, Cricetidae) en hábitats diferentes (pp. 935-947).
484   In: Salinas, P., editor. Actas de Séptimo Congreso Latinoamericano de Zoología,
485   Zoología Neotropical, Mérida, Venezuela.
486 González, L.A; Murúa, R. & Jofré, C. (2000) Habitat utilization of two muroid species in
487   relation to population outbreaks in southern temperate forests of Chile. Rev Chil Hist Nat.
488   73: 489-495.
489 Goudet, J. (1995) FSTAT version 1.2: a computer program to calculate F-statistics. J Hered.
490   86:485-486
491 Guilliot, G.; Mortier, F. & Estoup, A. (2005) Genelad: A computer package for landscape
492   genetics. Mol Ecol Notes. 5: 712-715.
493 Guilliot, G.; Santos, F. & Estoup, A. (2008) Analysing georeferenced population genetics data
494   with Geneland: A new algorithm to deal with null alleles and a friendly graphical user
495   interface. Bioinformatics. 24: 1406-1407.
496 Hall, T.A. (1999) BioEdit: a user-friendly biological sequence alignment editor and analysis
497   program for Windows 95/98/NT. Nucleid Acids Symp. Ser. 41: 95-98.
498 Harrison, S. (2004). The Pleistocene glaciations of Chile. Quaternary Glaciations–Extent and
499   Chronology. Part III: South America, Asia, Africa, Australasia, Antarctica, edited by:
500   Ehlers, J. and Gibbard, PL, Cambridge.
501 Himes, C.M.T.; Gallardo, M.H. & Kenagy, G.J. (2008) Historical biogeography and post-glacial
502   recolonization of South American temperate rain forest by the relictual marsupial
503   *Dromiciops gliroides*. J Biogeogr. 35: 1415-1424.
504 Holling, J.T. & Schilling, D.H. (1981) Late Wisconsin-Weichselian mountains glaciers and small
505   ice caps (pp 179-206). In: Denton, G.H. & Hughes, T.J. editors. The last great ice sheets.
506   John Wiley & Sons, New York, USA.
507 Iriarte, W.A. (2008) Mamíferos de Chile. Lynx edicions, Barcelona, España.
508 Kalinowski, S.T. (2005). hp-rare 1.0: a computer program for performing rarefaction on
509   measures of allelic richness. Mol Ecol Notes. 5: 187-189.
510 Kopelman, N.M.; Mayzel, J.; Jakobsson, M.; Rosenberg, N.A. & Mayrose, I. (2015). Clumpak: a
511   program for identifying clustering modes and packaging population structure inferences
512   across K. Mol Ecol Resour. 15: 1179-1191.

513   Lara, A.; Solari, M.E.; Prieto, M.R. & Peña, M.P. (2012) Reconstrucción de la cobertura de la

514   vegetación y uso del suelo hacia 1550 y sus cambios a 2007 en la ecorregión de los

515   bosques valdivianos lluviosos de Chile (35° - 40° 30' S). Bosque. 33: 13-23.

516   Larkin, M. A.; Blackshields, G.; Brown, N. P.; Chenna, R.; McGettigan, P. A.; McWilliam, H.;

517   ... & Thompson, J. D. (2007) Clustal W and Clustal X version 2.0. bioinformatics, 23:

518   2947-2948.

519   Leigh, J.W. & Bryant, D. (2015). popart: full-feature software for haplotype network

520   construction. Methods in Ecology and Evolution, 6: 1110-1116.

521   Mann, G. (1978). Los pequeños mamíferos de Chile: marsupiales, quirópteros, edentados y

522   roedores. Gayana Zoologia, 40: 1-342.

523   Manni, F.; Guérard, E. & Heyer, E. (2004). Geographic patterns of (genetic, morphologic,

524   linguistic) variation: how barriers can be detected by "Monmonier`s algorithm". Hum

525   Biol, 76:173-190.

526   Meirmans, P.G., & Van Tienderen, P.H. (2004). GENOTYPE and GENODIVE: two programs

527   for the analysis of genetic diversity of asexual organisms, Mol Ecol Notes 4: 792-794.

528   Mills, J.N.; Yates, T.L.; Childs, J.E.; Parmenter, R.R.; Ksiazek, T.G.; Rollin, P.E. & Peters, C.J.

529   (1995) Guidelines for working with rodents potentially infected with Hantavirus. J

530   Mammal. 76: 716-722.

531   Miranda, A.; Altamirano, A.; Cayuela, L.; Lara, A., & González, M. (2017). Native forest loss in

532   the Chilean biodiversity hotspot: revealing the evidence. Reg Environ Change. 1: 285-

533   297.

534   Mittermeier, R.A.; Robles Gil, P.; Hoffman, M.; Pilgrim, J.; Brooks, T.; Goettsch Mittermeier,

535   C.; Lamoreux, J. & da Fonseca, G.A.B. (2004). Hotspots Revisited: Earth's Biologically

536   Richest and Most Endangered Terrestrial Ecoregions. Cemex, Mexico City, Mexico.

537   Moreno, P.I.; Denton, G.H.; Moreno, H.; Lowell, T.V.; Putnam, A. E. & Kaplan, M.R. (2015).

538   Radiocarbon chronology of the last glacial maximum and its termination in northwestern

539   Patagonia. Quaternary Sci Rev. 122, 233-249.

540   Murúa, R. & González, L.A. (1982) Microhabitat selection in two Chilean cricetid rodents.

541   Oecologia. 52: 12-15.

542   Murúa, R. & González, L.A. (1986) Regulation of numbers in two Neotropical rodent species in

543   southern Chile. Rev. Chil. Hist. Nat. 59: 193-200.

544 Napolitano, C.; Johnson, W.W.; Sanderson, J.; O'Brien, S.J.; Rus Hoelzel, A.; Freer, R.; … &
545   Poulin, E. (2014) Phylogeography and population history of *Leopardus guigna*, the
546   smallest American felid. Conserv Genet. 15: 631-653.

547 Olson, D.M. & Dinerstein, E. (1998) The global 200: A representation approach to conserving
548   the Earth's most biologically valuable ecoregions. Conserv Biol. 12: 502-515.

549 Omote, K.; Nishida, C.; Takenaka, T., & Masuda, R. (2012). Temporal changes of genetic
550   population structure and diversity in the endangered Blakiston's fish owl (Bubo
551   blakistoni) on Hokkaido Island, Japan, revealed by microsatellite analysis. Zoo sci, 29:
552   299-304.

553 Osgood, W.H. (1943). The mammals of Chile, Vol. 30. University Chicago, Chicago.

554 Palma, R.E.; Rivera-Milla, E.; Salazar-Bravo, J.; Torres-Pérez, F.; Pardiñas, U.F.J; Marquet,
555   P.A. & Yates, T.L. (2005) Phylogeography of *Oligoryzomys longicaudatus* (Rodentia:
556   Sigmodontinae) in temperate South America. J Mammal. 86: 191-200.

557 Palma, R.E.; Boric-Bargetto, D.; Torres-Pérez, F.; Hernández, C.E. & Yates, T.L. (2012)
558   Glaciation effects on the phylogeographic structure of *Oligoryzomys longicaudatus*
559   (Rodentia: Sigmodontinae) in the Southern Andes. Plos One. 7: e32206.

560 Patterson, B. D., Meserve, P. L., & Lang, B. K. (1990). Quantitative habitat associations of small
561   mammals along an elevational transect in temperate rainforests of Chile. *Journal of
562   Mammalogy*, *71*: 620-633.

563 Patterson, B. D., P. Teta, and M F Smith. 2015 Genus Abrothrix Waterhouse, 1837. In Mammals
564   of South America, Vol. 2: Rodents. J.L. Patton, U.F.J. Pardiñas, and G. D'Elía, eds. Pp.
565   109-126. Chicago: University of Chicago Press.

566 Peakall, R. & Smouse, P.E. (2012). GenAlEx 6.5: genetic analysis in Excel. Population genetic
567   software for teaching and research—an update. Bioinformatics. 28: 2537-2539.

568 Pearson, O.P. & Smith, M.F. (1999). Genetic similarity between Akodon olivaceus and Akodon
569   xanthorhinus (Rodentia: Muridae) in Argentina. J Zoo. 247: 43-52.

570 Pritchard, J.K.; Stephens, M. & Donnelly, P. (2000) Inference of population structure using
571   multilocus genotype data. Genetics. 155: 945-959.

572 Rabassa, J. & Clapperton, C.M. (1990). Quaternary glaciations of the southern
573   Andes. Quaternary Sci Rev. 9: 153-174.

574   Rodríguez-Serrano, E.; Cancino, R.A. & Palma, R.E. (2006) Molecular phylogeography of
575   *Abrothrix olivaceus* (Rodentia: Sigmodontinae) in Chile. J Mammal. 87: 971-980.

576   Segovia, R. A., M. F. Pérez & L.F. Hinojosa (2012) Genetic evidence for glacial refugia of the
577   temperate tree *Eucryphia cordifolia* (*cunoniaceae*) in southern South America. Am J Bot.
578   99: 121–129

579   Sersic, A.N.; Cosacov, A.; Cocucci, A.A.; Johnson, L.A.; Pozner, R.; Avila, L.J.; Sites, J.W. &
580   Morando, M. (2011). Emerging phylogeographical patterns of plants and terrestrial
581   vertebrates from Patagonia.Biol J Linn Soc.103(2), 475-494.

582   Sikes, R.S. & Gannon, W.L. The animal care and use committee of the American Society of
583   Mammalogists. (2011) Guidelines of the American Society of Mammalogists for the use
584   of wild mammals in research. J Mammal. 92: 235-253.

585   Tajima, F. (1989) Statistical method for testing the neutral mutation hypothesis by DNA
586   polymorphism. Genetics. 123: 585-595

587   Van Oosterhout, C.; Hutchinson, W.F.; Wills, D.P. & Shipley, P. (2004). MICRO-CHECKER:
588   software for identifying and correcting genotyping errors in microsatellite data. Mol Ecol
589   Notes. 4: 535-538.

590   Veblen, T.T. (2007) Temperate forests of the Southern Andean region (pp. 217-231). In: Veblen,
591   T.T.; Orme, A.R. & Young, K.R., editors. The physical geography of South America.
592   Oxford University Press, Oxford, UK.

593   Vidal, M. A., Moreno, P. I., & Poulin, E. (2012a). Genetic diversity and insular colonization of
594   *Liolaemus pictus* (Squamata, Liolaeminae) in north-western Patagonia. Austral Ecol. 371:
595   67-77.

596   Vidal, M.A.; Ortiz, J.C.; Marín, J.C.; Poulin, E. & Moreno, P.I. (2012b) Comparative
597   phylogeography of two co-distributed species of lizars of the genus *Liolaemus*
598   (Squamata: Tropiduridae) from Southern Chile. Amphibia-Reptilia. 33: 55-67.

599   Vilà, C.; Leonard, J.A.; Iriarte, A.; O'Brien, S.J.; Johnson, W.E. & Wayne, R.K. (2004)
600   Detecting the vanishing populations of the highly endangered Darwin's fox,
601   *Pseudocalopex fulvipes*. Anim Conserv. 7: 147-153.

602   Yahnke, C.; Johnson, W.; Geffen, E.; Smith, D.; Hertel, F.; Roy, M.S.; Bonacic, C.; Fuller, T.K.;
603   Van Vulkenburgh, B. & Wayne, R.K. (1996) Darwin's Fox: A distinct endangered
604   species in a vanishing habitat. Conserv Biol. 10: 336-375.

605   Young, A.G., & Clarke, G.M. editors. (2000). Genetics, Demography and Viability of

606   Fragmented Populations. Cambridge University Press, Cambridge.

607
608
609
610
611
612
613
614
615
616
617
618
619
620
621
622
623
624
625
626
627
628
629   **Figure legends**:
630

631   Figure 1, Map of sampling sites; Study area in southern Chile, blue shade represents the Last

632   Glacial Maximum (LGM), green shade with black stripes in complete Chile indicates the

633   distribution of the Temperate Rainforest. On Chiloe Island in orange is delimitated the Cordillera

634   de Piuche. Black lines over the map indicates the result of the software Barriers, along with the

635   percentage of bootstrap of each barrier. The colors on the sampling point of the localities (study

636   area): Panguipulli (green), Valdivia (light blue), Bahia Mansa (gray), Las Quemas (Turquoise),

637   Senda Darwin (dark red), Cucao (Purple), Mininco (pink) and Alto Rio Ibañez (yellow);

638   represents localities that have mitochondrial sequences. Localities with light red color (Santa

639   Lucia, Palena and Rio Simpson) were only amplified for microsatellite markers.

640

641   Figure 2, Haplotype Network; Haplotype relationships of *A. olivacea brachiotis*. Each circle

642   represents a single haplotype sized in proportion of its frequency. The color code of each locality

643   is shown in the figure (BMLP; Bahía Mansa/La Picada and ARI; Alto Rio Ibañez).

644

645 Figure 3. Relationship between Nei`s genetic distance and geographical distance in km among

646 populations of *Abrothrix olivacea brachiotis* (Mantel test of correlation, rxy=0.386, p=0.01)

647

648 Figure 4, STRUCTURE analyses; Population structure of 187 individuals of *Abrothrix olivacea*

649 *brachiotis* inferred from Structure analyses. A) Structure with K=3, second highest probability.

650 B) Structure with K=4. C) Structure with K=5, highest probability with Evanno method.

651 Numbers represent the different sampling sites: 1 Panguipulli, 2 Valdivia, 3 Bahia Mansa, 4 La

652 Picada, 5 Las Quemas, 6 Senda Darwin, 7 Cucao, 8 Santa Lucia, 9 Palena, 10 Rio Simpson, 11

653 Mininco, 12 Alto Rio Ibañez.

654

655 Figure 5, Spatial population structure; GENELAND analyses with posterior probability isoclines.

656 Black dots represent the localities included in this study. Yellow indicates regions with the

657 greatest posterior probability of inclusion, and red areas show regions with the lower

658 probabilities of inclusion. Probabilities are proportional to the degree of coloring. A) Cluster

659 number 1 with populations of Valdivia, Bahia Mansa, Las Quemas, La Picada, Panguipulli and

660 Senda Darwin (Chiloe); B) Cluster number 2 with populations of Panguipulli and Cucao; C)

661 Cluster number 3 with populations of Santa Lucia, Palena, Rio Simpson, Mininco and Alto Rio

662 Ibañez.

663 **Table legends**:

664

665 Table 1, Genetic diversity; N, Number of individuals, H_o, observed heterozygosity; H_S, expected

666 heterozygosity; A, Number of alleles; Ar, Number of alleles with rarefaction (20 genes); G_{IS},

667 Inbreeding coefficient; Ne, Effective population size. The two upper columns represent the

668 grouping per sampling localities and per genetic clusters (according to Structure analysis).

669

670

671

672

673 **Supplementary Material**

674   Table S1. Localities sampled; List of specimens analyzed and geographic coordinates, with the

675   genetic marker used (Microsatellite STR and/or mitochondrial)

676   Table S2. GenBank accessions for microsatellite primer sets.

677   Table S3, Pairwise differentiation F_{ST}; Pairwise comparison between population above the

678   diagonal and p values below the diagonal. (* = p > 0.01)

679

Figure 1

Map of sampling sites

Study area in southern Chile, blue shade represents the Last Glacial Maximum (LGM), green shade with black stripes in complete Chile indicates the distribution of the Temperate Rainforest. On Chiloe Island in orange is delimitated the Cordillera de Piuche. Black lines over the map indicates the result of the software Barriers, along with the percentage of bootstrap of each barrier. The colors on the sampling point of the localities (study area): Panguipulli (green), Valdivia (light blue), Bahia Mansa (gray), Las Quemas (Turquoise), Senda Darwin (dark red), Cucao (Purple), Mininco (pink) and Alto Rio Ibañez (yellow); represents localities that have mitochondrial sequences. Localities with light red color (Santa Lucia, Palena and Rio Simpson) were only amplified for microsatellite markers.
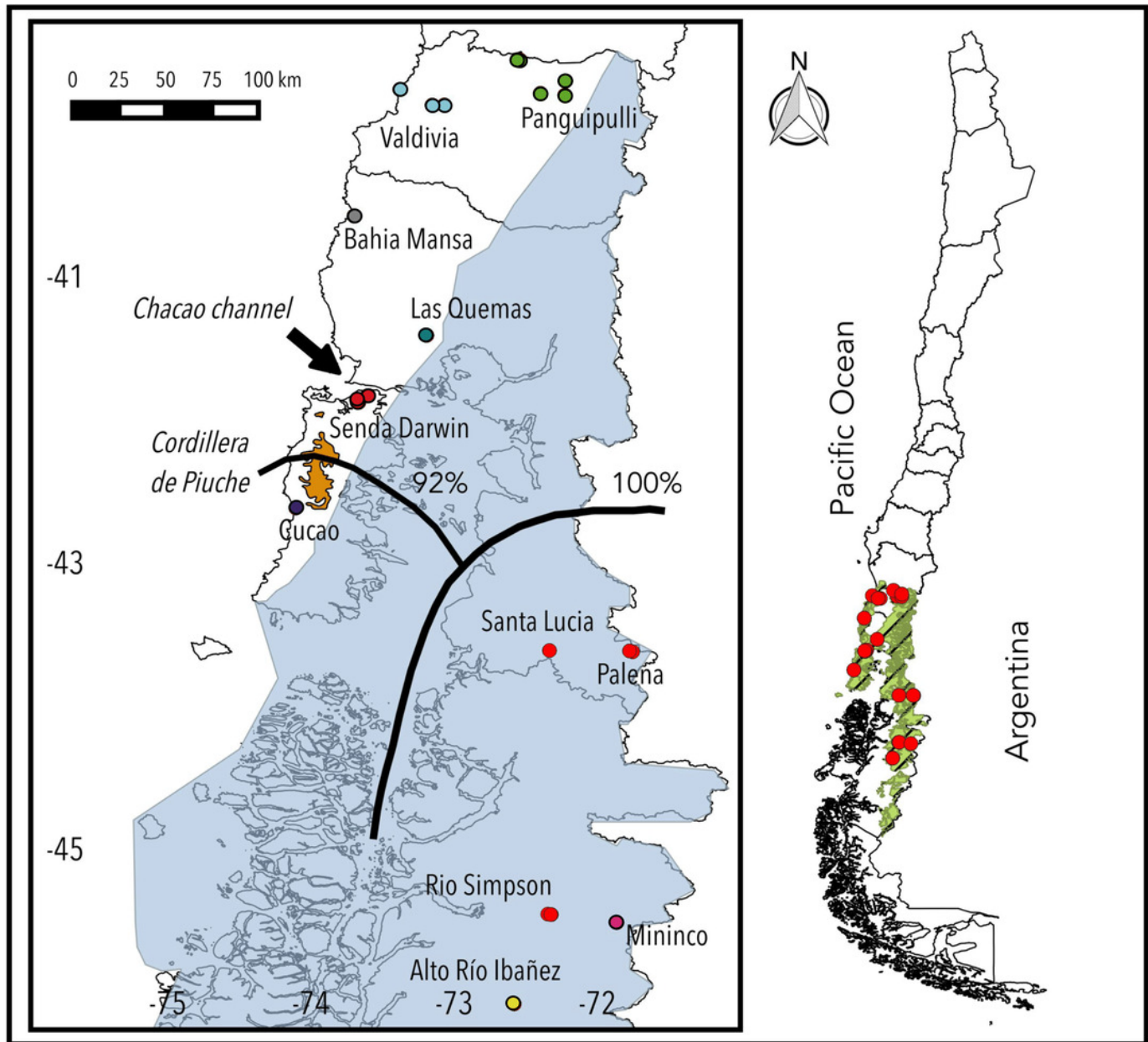
Map figure showing sampling locations in southern Chile including Valdivia, Panguipulli, Bahia Mansa, Las Quemas, Chacao channel, Senda Darwin, Cordillera de Piuche, Cucao, Santa Lucia, Palena, Rio Simpson, Mininco, and Alto Río Ibañez, with labels 92% and 100%, and an inset map of Chile showing the Pacific Ocean and Argentina.

Figure 2

Haplotype Network

Haplotype relationships of *A. olivacea brachiotis*. Each circles represent a single haplotype sized in proportion of its frequency. The color code of each locality its shown in the figure (BMLP; Bahía Mansa and ARI; Alto Rio Ibañez).
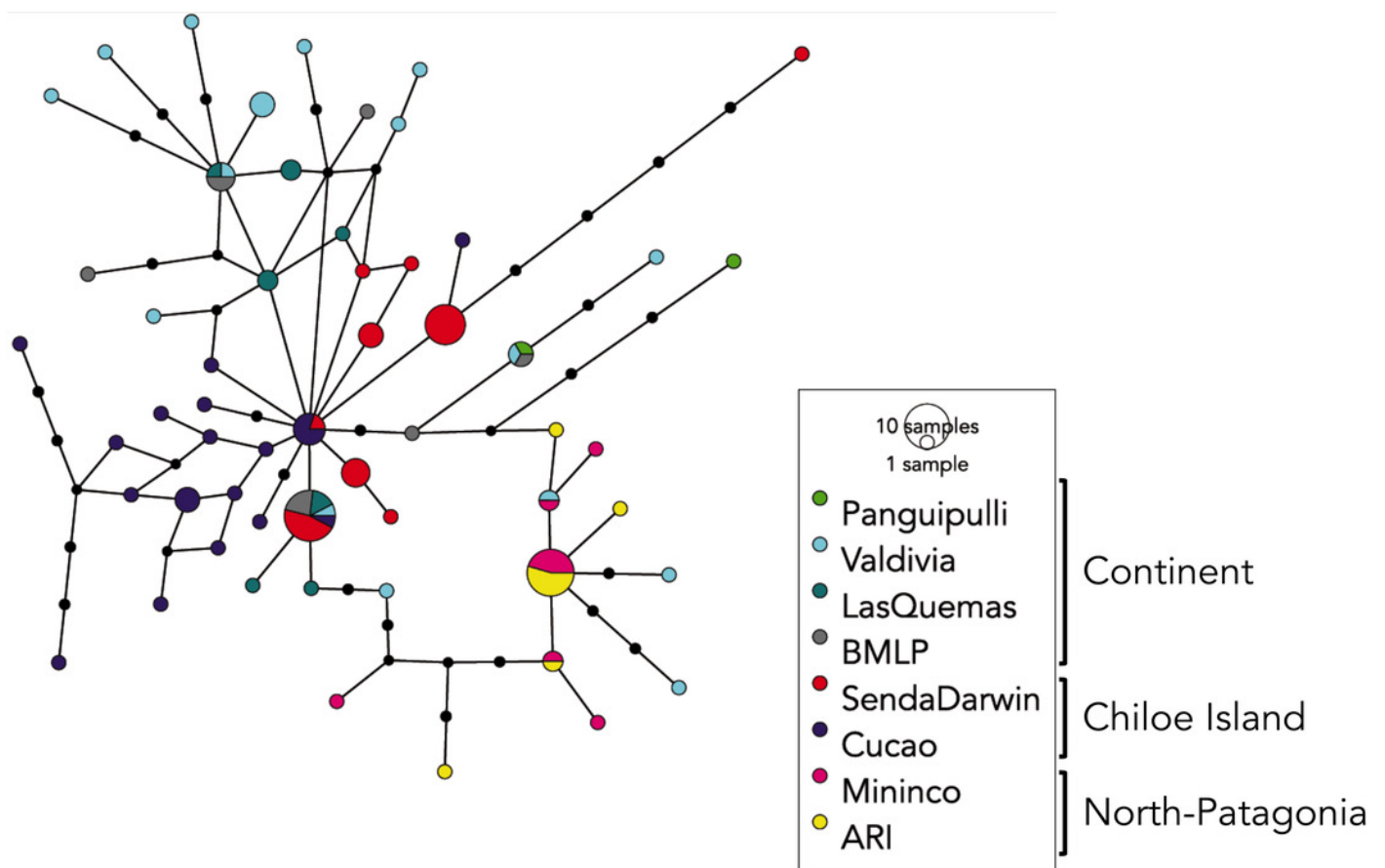
Figure 3

Mantel test

Relationship between Nei`s genetic distance and geographical distance in km among populations of *Abrothrix olivacea brachiotis*(Mantel test of correlation, rxy=0.386, p=0.01)
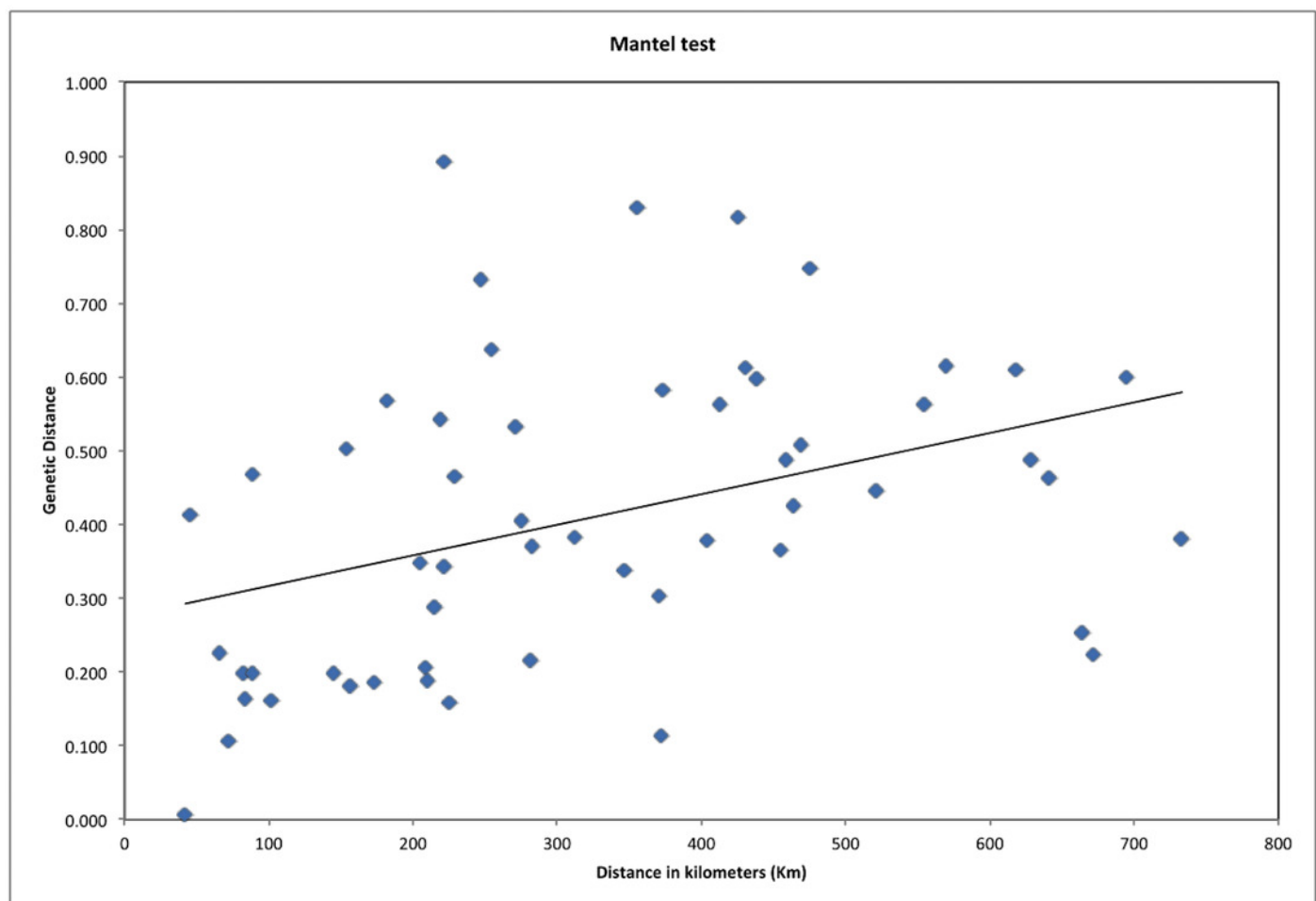
Figure 4

STRUCTURE analyses

Population structure of 187 individuals of *Abrothrix olivacea brachiotis* inferred from Structure analyses. A) Structure with K=3, second highest probability B) Structure with K=4 C) Structure with K=5, highest probability with Evanno method. Numbers represent the different sampling sites: 1 Panguipulli, 2 Valdivia, 3 Bahia Mansa, 4 La Picada, 5 Las Quemas, 6 Senda Darwin, 7 Cucao, 8 Santa Lucia, 9 Palena, 10 Rio Simpson, 11 Mininco, 12 Alto Rio Ibañez.
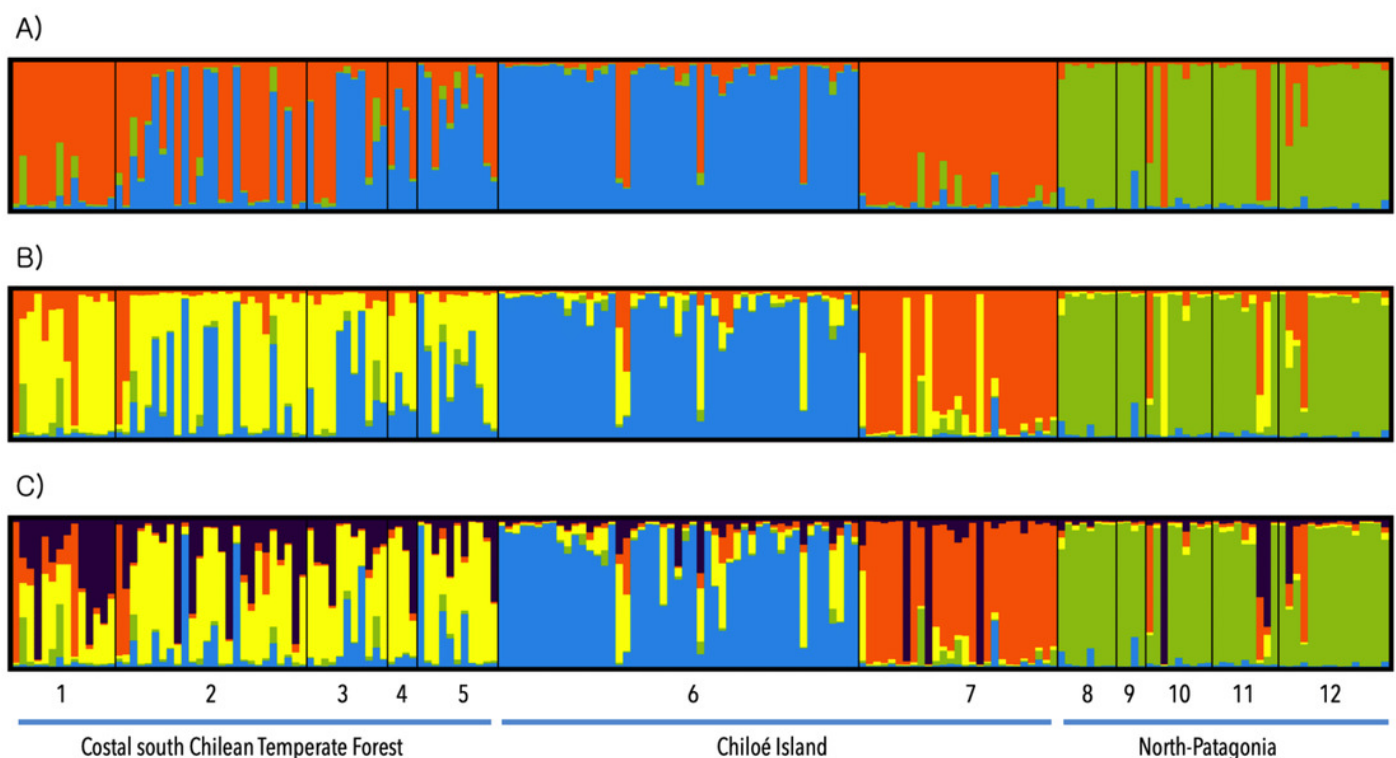
Figure 5

Spatial population structure

GENELAND analyses with posterior probability isoclines. Black dots represent the locality presents in this study. Yellow indicates regions with he greatest posterior probability of inclusion, and red areas shows region with lower probabilities of inclusion, this proportional to the degree of coloring. A) Cluster number 1 with populations of Valdivia, Bahia Mansa, Las Quemas, La Picada, Panguipulli and Senda Darwin (Chiloe); B) Cluster number 2 with populations of Panguipulli and Cucao; C) Cluster number 3 with populations of Santa Lucia, Palena, Rio Simpson, Mininco and Alto Rio Ibañez.
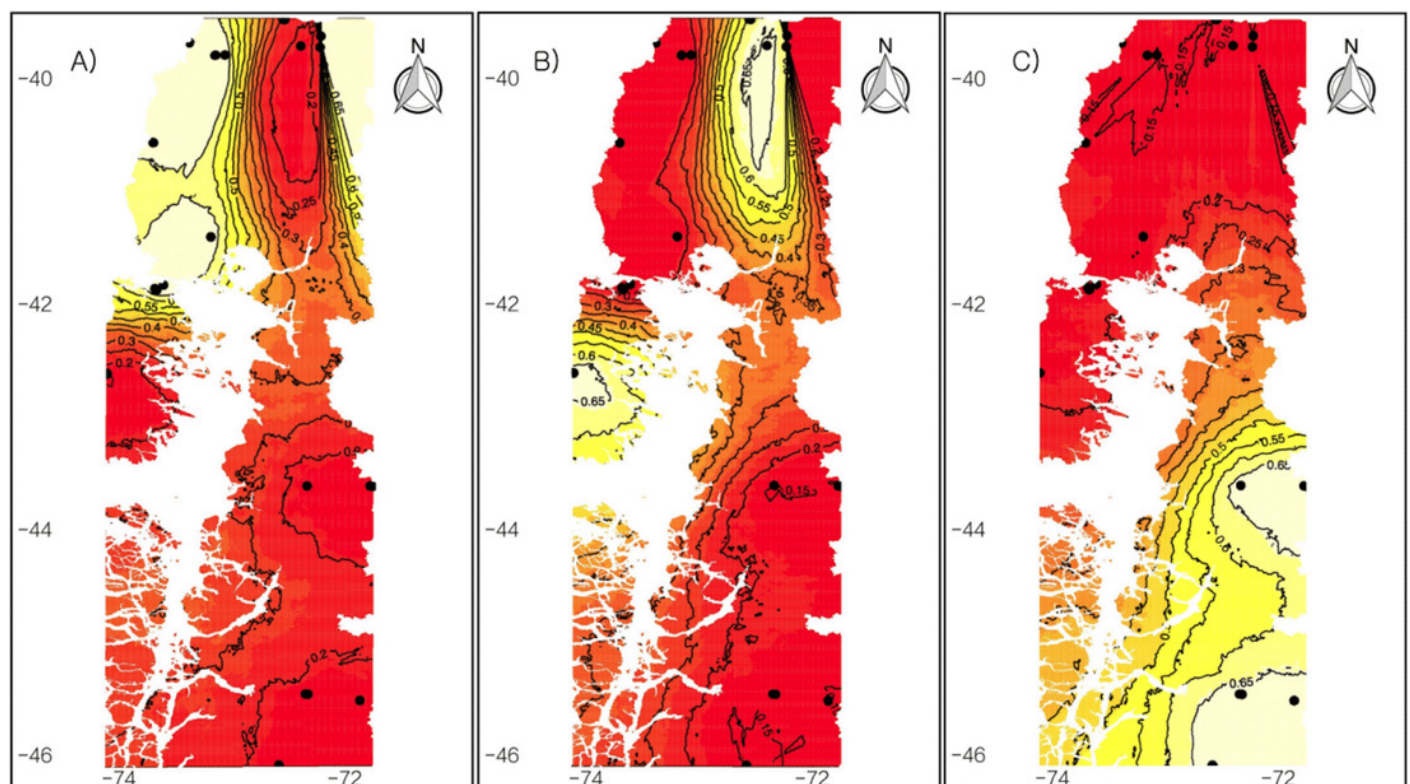
Genetic diversity

N, Number of individuals, H_o, observed heterozygosity; H_s, expected heterozygosity; A, Number of alleles; Ar, Number of alleles with rarefaction (20 genes); G_{IS}, Inbreeding coefficient; Ne, Effective population size. The two upper columns represent the grouping per sampling localities and per genetic clusters (according to Structure analysis).

1   Table 1

	Sampling locations				Genetic clusters						
Population	N	Ho	He	A	Ar	N	A	Ar	Ho	Hs	Gis	Ne
Panguipulli	14	0.835	0.887	12.33	10.45	66	20.75	10.53	0.776	0.878	0.117	683.3 (313.9 − ∞)
Valdivia	26	0.79	0.865	14.83	10.09							
Bahia Mansa (BH_M)	11	0.718	0.844	7.67	7.2							
La Picada	4	0.562	0.844	4.33	4.33							
Las Quemas	11	0.775	0.84	9.75	8.57							
Senda Darwin	49	0.748	0.809	17	8.7	49	17	8.7	0.748	0.809	0.076	274.9 (164.1 − 762.1)
Cucao	27	0.848	0.979	14.33	9.49	27	14.33	9.49	0.843	0.879	0.041	54 (41.1 − 76.4)
Palena Santa Lucia	12	0.735	0.78	7.5	6.08	45	15.66	9.13	0.759	0.825	0.08	113.2 (82.4 − 174.4)
Rio Simpson	9	0.749	0.831	8.08	8.08							
Mininco	9	0.762	0.829	7.67	7.5							
Alto Rio Ibañez	15	0.771	0.771	8.42	7.5							